Composition and Temperature Dependence of the Segmental Interaction Parameter in Statistical Copolymer/Homopolymer Blends

D. W. Schubert,*,† V. Abetz,*,‡ M. Stamm,† T. Hack,† and W. Siol§

Max-Planck-Institut für Polymerforschung, Postfach 3148, 55021 Mainz, Germany, Institut für Organische Chemie, Johannes Gutenberg-Universität Mainz, Postfach 3980, 55099 Mainz, Germany, and Röhm GmbH, Postfach 4242, 64201 Darmstadt, Germany

Received July 9, 1994; Revised Manuscript Received December 22, 1994®

ABSTRACT: The polymer blend system of deuterated polystyrene (PS(D)) and a statistical copolymer poly(cyclohexyl acrylate-*stat*-*n*-butyl methacrylate) (P(CHA_{1-x}-*stat*-nBMA_x)) was investigated by small-angle neutron scattering (SANS) and neutron reflectometry (NR). The Flory–Huggins–Staverman interaction parameter χ was determined as a function of temperature and copolymer composition in the one- and two-phase regions by SANS and NR, respectively. By a combination of both methods compatible and incompatible blends could be investigated. It is shown that theoretical treatments of the two regimes are consistent. The phase diagram is calculated where a switching from an upper critical solution temperature to a lower critical temperature behavior is predicted.

Introduction

The understanding of compatibility between different polymers is one of the major problems in the field of polymer blends. Much experimental and theoretical work has been done in order to get insight into the quantities controlling the phase behaviour of polymer blends.[1–9]

Only a few examples are known, where two homopolymers are miscible. Statistical copolymers, on the other hand, may be tuned to show miscibility with homopolymers or other statistical copolymers.[5] Well-known examples are blends of poly(styrene-*stat*-acrylonitrile) and poly(styrene-*stat*-maleic anhydride)[8] or blends of poly(methyl methacrylate) and poly(styrene-*stat*-acrylonitrile)[9] for the first and second kinds of blends, respectively. In both of these examples none of the basic homopolymers are compatible with the other component. The induced compatibility can be understood in terms of the different contributions of segment interaction to the Flory–Huggins–Staverman χ-parameter and is called the $\Delta\chi$ effect, as first described for ternary polymer solutions by Patterson.[10] Miscibility can also be achieved by a combination of monomers A and B in a statistical copolymer P(AB), when at least one of them is miscible with the other component C, which is used in the present system.

While scattering techniques like small-angle X-ray or neutron scattering (SAXS, SANS) as well as light scattering have been applied in numerous cases for the study of phase behaviour and decomposition kinetics of polymer blends, the technique of neutron reflectometry (NR) has only been applied in some selected cases for the determination of segmental interaction in polymer blends.[11–13] Examples are blends of poly(vinyl chloride) with poly(methyl methacrylate) (PMMA)[14] or poly(vinyl methyl ether) with polystyrene (PS).[15] In those cases initial stages of interdiffusion at an interface can be followed, since NR has good sensitivity only for interface widths typically smaller than 15 nm.[12] It thus is in particular also an ideal technique for the investigation of incompatible polymer blends where the equilibrium interface width is typically in the range between 1 and 15 nm depending on the compatibility of the components. Examples of those investigations by NR are the systems PS versus PMMA[16] or PS versus poly(styrene-*stat*-*p*-bromostyrene),[17] where in the latter case compatibility can be tuned by the degree of bromination in the statistical copolymer.

In this study we examine the χ-parameter in blends containing 50 wt % deuterated polystyrene (PS(D)) and 50 wt % poly(cyclohexyl acrylate-*stat*-*n*-butyl methacrylate) (P(CHA_{1-x}-*stat*-nBMA_x)) as a function of the composition x of the statistical copolymer. PS(D) is used in order to achieve good contrast for neutron scattering experiments. This system shows a strong variation of miscibility with the composition of the copolymer. While poly(cyclohexyl acrylate) is miscible with PS(D) in a large temperature range at all concentrations, poly(*n*-butyl methacrylate) is miscible with PS(D) only in the case of small molecular weights, i.e., if the entropy of mixing is able to balance the strong repulsive enthalpic interactions.

Here we use a combination of two different experimental techniques in order to examine both the miscible and immiscible polymer blends. While the miscible blends were studied by SANS, in the case of immiscible blends NR was used for the determination of the interface between the two polymers. From both experiments we can obtain the segmental interaction parameter χ, which thus can be determined over a wide composition range.

Experimental Section

Samples for Small-Angle Neutron Scattering. PS(D)-1 was obtained via anionic polymerization (Max-Planck-Institut für Polymerforschung). The copolymers were specifically made by radical polymerization (Röhm GmbH, Darmstadt). The composition of the copolymers was determined by ^1H NMR; the absolute molecular weights (weight-average molecular weight M_w) were obtained by light scattering in tetrahydrofuran. Polydispersities were determined by gel permeation chromatography (GPC) using PMMA calibration for the copolymers and PS calibration for PS(D). The molecular characteristics are given in Table 1.

* Authors to whom correspondence should be addressed.
† Max-Planck-Institut für Polymerforschung.
‡ Johannes Gutenberg-Universität Mainz.
§ Röhm GmbH.
® Abstract published in *Advance ACS Abstracts,* March 1, 1995.

0024-9297/95/2228-2519$09.00/0

Table 1. Molecular Characteristics of the Polymers

polymer	M_w (kg/mol)	M_w/M_n	N
PS(D)-1	99	1.07	885
PS(D)-2	720	1.13	5670
PnBMA	150	1.03	1355
PCHA	465	2.85	4344
P(CHA$_{0.61}$-*stat*-nBMA$_{0.39}$)	423	1.84	3952
P(CHA$_{0.39}$-*stat*-nBMA$_{0.61}$)	415	1.88	3877
P(CHA$_{0.36}$-*stat*-nBMA$_{0.64}$)	274	1.73	2561
P(CHA$_{0.32}$-*stat*-nBMA$_{0.68}$)	265	1.81	2476

The degrees of polymerization N are calculated from M_w based on the monomer volume of styrene. This means that the chemical degrees of polymerization were corrected by a factor accounting for the different monomeric volumes of styrene (99.378 cm^3/mol), cyclohexyl acrylate (142.989 cm^3/mol), and *n*-butyl methacrylate (131.847 cm^3/mol). The corresponding volumes were calculated from tabulated densities at 20 °C.[18]

To obtain blends of a concentration $\phi = 0.5$, the components were dissolved in THF (5 wt %) and cast into a Petri dish. The solvent was evaporated at room temperature under normal pressure for 24 h. Then the samples were put into an oven and dried at 130 °C under normal pressure for 24 h. Afterward the oven was put under vacuum for another 24 h. Pellets with a thickness of around 0.6−1 mm and a diameter of 13 mm were obtained by melt pressing (T_g + 40 K, 5 kN) for 0.5 h.

The glass transition temperature, T_g, of the blends at 50% composition is almost independent of the copolymer composition ($T_g \cong 55$ °C, as obtained by differential scanning calorimetry with a heating rate of 10 K/min).

Sample for Neutron Reflectometry. PS(D)-2 and PnBMA synthesized via anionic polymerization with narrow molecular weight distributions as determined by GPC were obtained from PSS (Mainz). The molecular characteristics are given in Table 1.

Each polymer was dissolved in toluene at a concentration of about 2 wt % and then deposited by spin coating at a velocity of 2000 rpm onto float glass plates (100 × 100 mm^2). This method provides very smooth films with thicknesses of about 100 nm. The roughnesses of the single films were characterized by phase interference microscopy and X-ray reflectometry.[11] Subsequently, a PS(D)-2 layer was floated off onto water and picked up by a PnBMA film still deposited on a glass substrate. The bilayer film was dried for 2 days under vacuum at room temperature.

Small-Angle Neutron Scattering Measurements. Measurements were performed at the SANS instrument of Risø National Laboratory, Denmark. The sample was placed in a self-built oven, which was originally designed for temperature jump experiments. The sample in the oven can be purged with nitrogen, while the oven itself is placed in the vacuum tube of the neutron beam line. By keeping the sample at pressure slightly above 1 atm (by a balloon filled with nitrogen), the appearance of trapped air bubbles in the molten sample at higher temperatures could be suppressed. The wavelength of the neutrons was λ = 10.4 Å, and the distance of the two-dimensional ^{3}He detector from the sample was 6 m. This corresponds to a range of the scattering vector from 0.05 to 0.3 nm^{-1}. Temperature control was achieved to ±1 K. Since all the samples were isotropic, data were radially averaged for reduction of the experimental noise. Data were corrected for electronic background, scattering by the sample holder, transmission, and sample volume as well as for incoherent scattering by subtraction of the scattering profiles of the pure components by standard procedures. Calibration of the scattering profiles were done with the well-known differential scattering cross section of a water sample.

Neutron Reflectometry Measurements. The NR measurements presented in this work were carried out at TOREMA II, GKSS, Geesthacht, Germany, where the wavelength is fixed to 0.43 nm (graphite monochromator) and the angle of incidence of the neutrons at the sample is varied in the range between 0.1° and 1.5°. The beam collimation is achieved by two slits of width 0.45 and 0.70 mm at a distance of 174 cm. The reflected beam is detected with a position-sensitive BF_3 detector. Reflectivities down to approximately 10^{-4} were reached with typical run times of 12 h. Figure 1 shows a schematic picture of the sample and the characteristic parameters which define the refractive index profile. Details of data analysis will be described below.

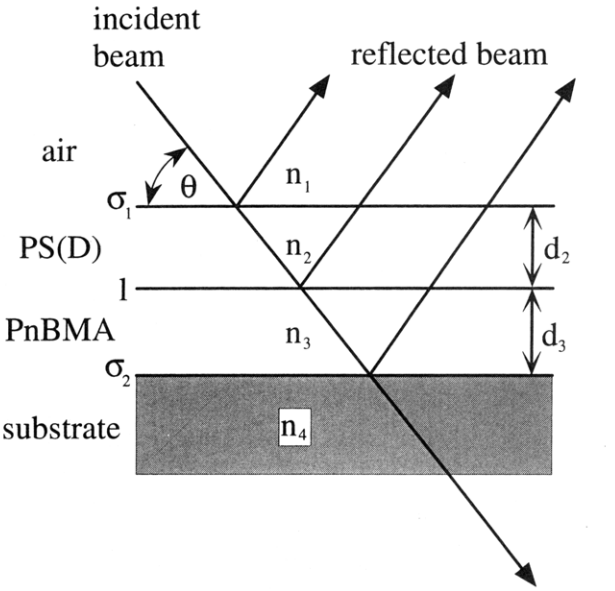

Figure 1. Schematic diagram of a neutron reflection experiment from a layered sample. Parameters are explained in the text.

Results and Discussion

Small-Angle Neutron Scattering. The free energy F of a system containing long-wavelength concentration fluctuations with small amplitudes is given by the following functional:[19,20]

$$\frac{F}{kT} = \int_0^\infty F_{FHS} + \frac{a^2}{36\phi(1-\phi)}\left(\frac{\partial\phi}{\partial r}\right)^2 dr \qquad (1)$$

where a is the average segment length, r the radial coordinate for isotropic volume, ϕ the volume fraction of component 1, F_{FHS} the Flory−Huggins−Staverman free energy of mixing, k Boltzmann's constant, and T the temperature. F_{FHS} is given by:[19−23]

$$F_{FHS} = \frac{\phi}{N_1}\ln\phi + \frac{1-\phi}{N_2}\ln(1-\phi) + \chi\phi(1-\phi) \qquad (2)$$

where χ is the Flory−Huggins−Staverman segmental interaction parameter and N_i the degree of polymerisation of component i. In this equation we neglect a possible concentration dependence of the χ-parameter. This is reasonable here, because all blends under investigation have the same concentration. Since we are discussing in the case of the SANS experiments only measurements in the single-phase region, we deal always only with weight averages of the degree of polymerization N and z-averages of the segmental length a. The polydispersity itself must not be taken into account in the single-phase region. In the case of phase separation, however, fractionation effects may become important, and for that reason polydispersity has to be taken into account.[24] Equation 1 is valid for $qR_g < 1$, with $R_g = (1/6)Na^2$ being the radius of gyration and q being the scattering vector ($q = (4\pi/\lambda)\sin(\delta)$,

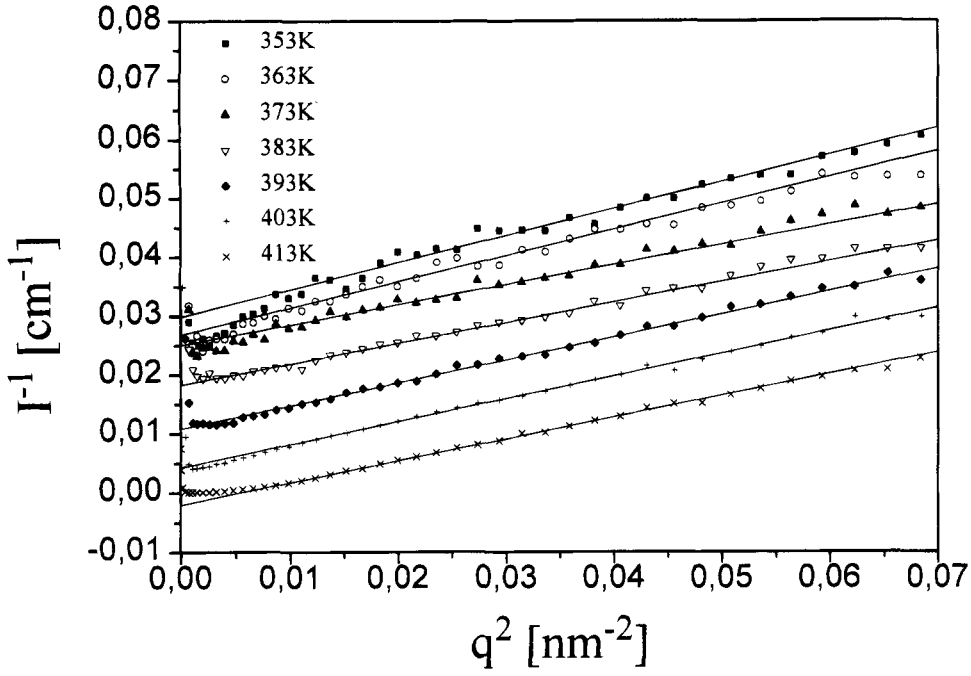

Figure 2. Zimm plot of SANS data of a P($CHA_{0.36}$-*stat*-n$BMA_{0.64}$)/PS(D)-1 blend at various temperatures. The solid lines represent linear fits based on eq 3.

where λ = wavelength of the neutrons and 2δ = scattering angle).

The inverse structure factor is the Fourier transform of the second derivative of the free energy functional and can be written in the Zimm approximation ($qR_g < 1$) as:

$$\frac{1}{S(q)} = \frac{1}{N_1\phi} + \frac{1}{N_2(1-\phi)} - 2\chi + \frac{a^2q^2}{18\phi(1-\phi)} \quad (3)$$

In the limit $q = 0$ eq 3 becomes identical to the second derivative of the normalized Flory–Huggins–Staverman free energy with respect to concentration.

The structure factor $S(q)$ is related to the measured intensity $I(q)$ in SANS experiments at small q by the following general relation:

$$I(q) = Kv_1S(q) \quad (4)$$

where K is the contrast factor ($K = (B_1/v_1 - B_2/v_2)^2$), B_i the neutron scattering length of monomer i, and v_i the volume of monomer i. Typical Zimm plots at different temperatures are shown in Figure 2 for P($CHA_{0.36}$-*stat*-n$BMA_{0.64}$)/PS(D)-1. The segment length a, obtained from the slope of the fitted straight lines in the different Zimm plots of the different samples studied, varies in a rather broad range (±0.2 nm) around an average value of 0.84 nm. However, variations in the slope of a linear fit in the Zimm plot using eq 3 do not significantly change the χ-parameter obtained from the intercept at $q = 0$; i.e., the intercept is not very sensitive to changes in a. This is due to the close neighborhood between the intercept and the data points, where the data must be fitted in order to fulfill the condition ($qR_g < 1$).

Figure 3 shows the χ-parameter as a function of reciprocal temperature for P($CHA_{0.36}$-*stat*-n$BMA_{0.64}$)/PS(D)-1. A linear fit describes the data quite well:

$$\chi = A + B/T \quad (5)$$

The deviations at low temperatures are probably due to the proximity of the glass transition temperature; i.e., the system was maybe not completely in thermodynamic equilibrium when being measured. Since the measurements at 90 and 80 °C were performed after the measurement at 100 °C, the values obtained for the χ-parameter from these two lower temperature measurements still resemble the sample at a higher temperature and have been skipped from the analysis. The fit parameters for the different blends according to eq 5 are listed in Table 3.

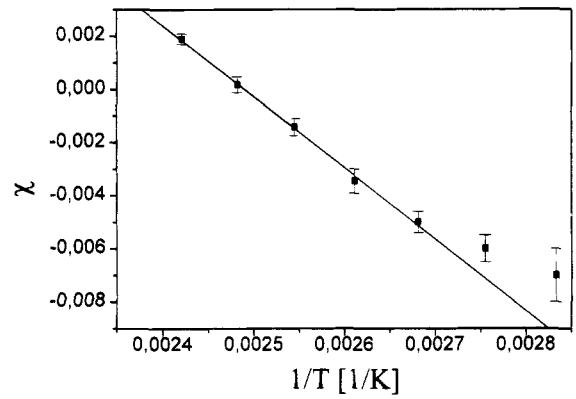

Figure 3. χ-Parameter as a function of inverse temperature for P($CHA_{0.36}$-*stat*-n$BMA_{0.64}$)/PS(D)-1. The solid line represents a fit for the temperature dependence of χ according to eq 5 with the parameters given in Table 3.

Neutron Reflectometry. The reflectivity of a multilayer system as shown in Figure 1 is determined by the profile of refractive index n assumed to vary only in the direction z perpendicular to the interfaces. Interface profiles of any form can be approximated by a sequence of thin homogeneous layers. By use of a matrix formalism,[25] reflectivities of such a multilayer system can then be calculated. Neglecting absorption, the refractive index for neutrons traveling in a medium of homogeneous scattering density is given by:

$$n = 1 - \frac{\lambda^2}{2\pi}N_A\sum_i \frac{\varrho_i}{A_i}b_i \quad (6)$$

Table 2. Fit Parameters for the NR Sample of PnBMA/PS(D)[a]

T (K)	σ_1 (nm)	σ_2 (nm)	d_2 (nm)	d_3 (nm)	l (nm)
393	0.9	0.9	167.8	86.3	3.2
410	0.9	0.9	167.8	86.3	3.6
420	0.9	0.9	167.8	86.3	3.9
429	0.9	0.9	167.8	86.3	4.3

[a] T = temperature. σ_1, σ_2 = variances of the error functions to describe roughness of the interfaces air/PS(D)-2 and PnBMA/glass, respectively. d_2 = thickness of the PS(D)-2 layers. d_3 = thickness of the PnBMA layer. l = interface width of the PS(D)-2/PnBMA interface.

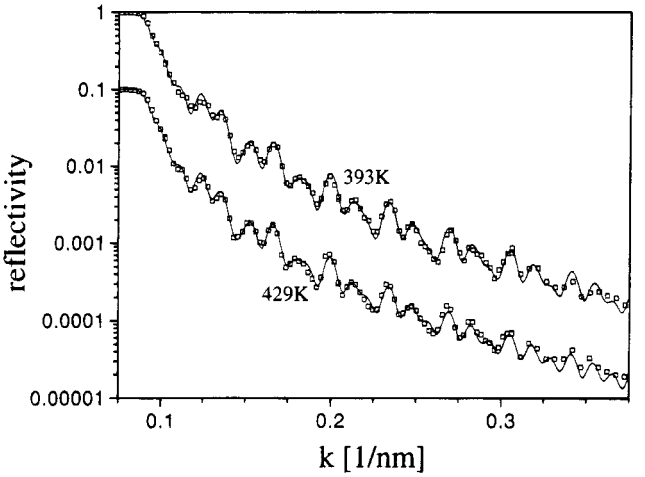

Figure 4. Neutron reflectivity data versus momentum transfer k for two different temperatures 393 and 429 K of the bilayer system PnBMA/PS(D)-2. The solid lines correspond to calculated fit curves. Open squares are measured reflectivities.

where N_A is Avogadro's number, ϱ_i the density, b_i the scattering length, and A_i the atomic weight of species i. The measured reflectivity is a function of the momentum transfer k perpendicular to the surface given by

$$k = (2\pi/\lambda) \sin \theta \tag{7}$$

and related to the angle of incidence θ. Comparison of the experimentally observed reflectivity curve with the calculated curve gives information about the refractive index profiles. Minimizing the deviation between experimental and calculated curves gives values for interfacial profiles and thicknesses of the individual layers with an accuracy of up to 0.1 nm. While NR fits in some cases produce nonunique results,[12] the fits in the present case are perfectly defined since the starting values for the layer thicknesses d_2 and d_3, the corresponding indices of refraction n_2 and n_3, and roughnesses of the interfaces air/polymer layer 2 and glass/polymer layer 3 expressed through the variances σ_1 and σ_2 of an error function profile (see Figure 1 and Table 2) are measured by X-ray reflectometry on the individual films and substrate, respectively. Those parameters are input into the fit, leaving essentially the interface width l between the two polymer layers as a free parameter which will be discussed below.

Figure 4 shows two different NR measurements and the reflection curves calculated with a model for the refractive index profile defined by the characteristic parameters shown in Table 2.

The interfaces air/PS(D)-2 and PnBMA/glass are described by error functions which are characterized by their variances σ_1 and σ_2. For the interface between the two polymers, a tanh refractive index profile is used, which is based on the profile for the volume fraction ϕ of one component in the interfacial region according to eq 8.[19] This profile is expected only for simple cases at the interface of polymer blends,[12] while generally deviations are expected. These originate, for instance, from a concentration dependence of χ or the limited validity of the used approximations in deriving eq 8.[26,27]

$$\phi = \frac{1}{2}\left(1 + \tanh\left(\frac{z}{l_t}\right)\right) \tag{8}$$

To obtain the true interfacial thickness l_t, an initial roughness l_0 of the interface before the annealing process is taken into account.[28] Assuming superposition of the two effects, the experimental interface width l can be obtained by convoluting the initially rough profile characterized by l_0 and the true interface profile l_t,

$$l^2 = l_t^2 + l_0^2 \tag{9}$$

where l_0 = 1.2 nm is taken to be constant during the annealing process. Initial, true, and experimental profiles can be approximated by the form of eq 8. It should be noted that the error function is quite similar to the tanh profile in eq 8. There is only a factor of approximately 1.2 between the variance σ and the characteristic parameter l. Regarding σ_1 and σ_2 in Table 2, one can see a constant roughness during the annealing process which is of the same origin as l_0. Conformational effects or thermal fluctuations at the interface as discussed recently[26] are neglected here. The measurements at different temperatures were done by annealing the sample at a specific temperature for a few hours and then quenching it to room temperature, where NR experiments were performed. It was checked that an equilibrium for the interface width was reached under these conditions by experiments at different annealing times.

The interface width obtained from NR can be directly related to the Flory–Huggins–Staverman χ-interaction parameter. A theoretical approach within the mean-field picture to describe the interface of an incompatible polymer blend is the minimization of the functional for the free energy:[20]

$$\frac{F}{kT} = \int_{-\infty}^{+\infty} F_{FHS} + \frac{a^2}{24\phi(1-\phi)}\left(\frac{\partial\phi}{\partial z}\right)^2 dz = \text{Min} \tag{10}$$

Parameters have the same meaning as in eq 1 with the exception that z now is a coordinate perpendicular to the interface. The prefactor in the gradient term is larger by a factor of $^3/_2$ as compared to the one in eq 1. This is due to the fact that eq 10 is an approximation for a small interface width, where $qR_g > 1$; i.e., it describes interface thicknesses in the range of the radii of gyration or even smaller. The boundary conditions in eq 10 to be satisfied are

$$\phi = 0; \quad \partial\phi/\partial z = 0 \qquad \text{for } z = -\infty \tag{11}$$

and

$$\phi = 1; \quad \partial\phi/\partial z = 0 \qquad \text{for } z = +\infty \tag{12}$$

For the case of $N_i \to \infty$, the hyperbolic tangent profile (eq 8) is an exact solution of eq 10 with the condition of eq 13.

$$l_t = a/(6\chi)^{1/2} \tag{13}$$

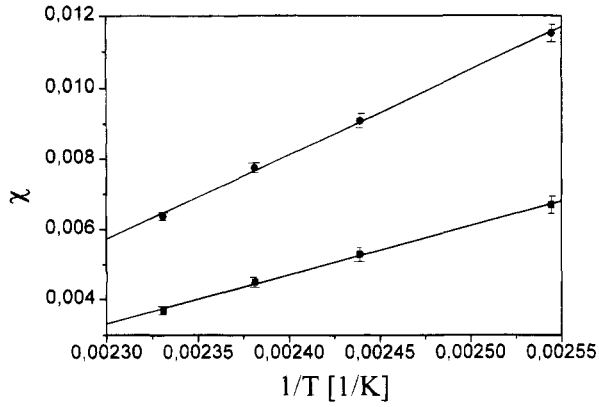

Figure 5. χ-Parameter as a function of inverse temperature for PnBMA/PS(D)-2 (a = 0.64 nm (■), a = 0.84 nm (●)). The solid lines correspond to linear fits according to eq 5, respectively.

Table 3. Composition Dependence of the Enthalpic (B) and Entropic Part (A) of the Interaction Parameter According to Equation 5

method	x_{nBMA}	A	B (K)
SANS	0.00	0.107 ● 0.008	−57 ± 3.6
SANS	0.39	0.095 ± 0.005	−45.6 ± 1.8
SANS	0.61	0.062 ± 0.007	−25.8 ± 2.5
SANS	0.64	0.067 ± 0.007	−26.8 ± 2.0
SANS	0.67	0.054 ± 0.005	−20.8 ± 2.0
NR	1.00		
a = 0.64 nm		−0.0357 ± 0.0009	17.7 ± 0.4
a = 0.84 nm		−0.0626 ± 0.0016	30.5 ± 0.7

For the general case we calculate the influence of N_1 and N_2 on the interface width (eq 14), using the hyperbolic tangent profile (eq 8) as a trial function to minimize eq 10. This yields

$$l_t = \frac{a}{\sqrt{6}}\left(\chi - \frac{\pi^2}{6}(N_1^{-1} + N_2^{-1})\right)^{-1/2} \quad (14)$$

It should be noted that other authors (for example, ref 19) obtain different prefactors in eqs 13 and 14 instead of $1/\sqrt{6}$. This is due to the different prefactor of the square gradient term in eq 10 (as compared to eq 1), where care has to be taken with respect to the used range and approximations. Equations 13 and 14 are thus valid for $qR_g > 1$ as mentioned before.

From eq 14 it follows, that the χ-parameter strongly depends on the mean segment length a. From the SANS measurements there is no clear evidence for a dependence of the mean segment length on the copolymer composition, due to the large error in the Zimm plots. A value given in the literature for this system is a = 0.64 nm.[29] However, this value is smaller than a value given for poly(methyl methacrylate) a = 0.74 ± 0.3 nm[30] and for polystryene a = 0.68 nm.[31] To account for the uncertainty in the segment length, we calculated the Flory–Huggins–Staverman interaction parameter χ for a = 0.64 nm and for a = 0.84 nm using eq 14. The results for different temperatures are shown in Figure 5.

The temperature dependence of the interaction parameter can be well described by eq 5. The data show a clear indication for the presence of an upper critical solution temperature (UCST) for PS(D)-1/PnBMA obtained by extrapolation of the data to higher temperatures. For a similar blend with much smaller molecular weights and large polydispersities (as compared to our sample) both UCST and LCST (lower critical solution temperature) have been discussed recently.[32]

A fit of eq 5 to the data presented in Figure 4 yields A and B (see Table 3).

The χ-Parameter as a Function of Copolymer Composition. The interaction of a copolymer blend can be described in the same manner as for blends of homopolymers using an effective interaction parameter. This effective interaction parameter contains all different binary interactions between the different components and can be expressed through:[5]

$$\chi = x\chi_{S-nBMA} + (1-x)\chi_{S-CHA} - x(1-x)\chi_{CHA-nBMA} \quad (15)$$

where x is the fraction of nBMA in the copolymer and χ_{i-j} denotes the segmental interaction between monomers i and j.

Using

$$\chi_{S-nBMA} = A_1 + B_1/T$$
$$\chi_{S-CHA} = A_2 + B_2/T$$
$$\chi_{CHA-nBMA} = A_3 + B_3/T \quad (16)$$

we obtain

$$\chi = A(x) + B(x)/T \quad (17)$$

with

$$A(x) = A_2 + x(A_1 - A_2 - A_3) + x^2A_3$$
$$B(x) = B_2 + x(B_1 - B_2 - B_3) + x^2B_3 \quad (18)$$

There is a good agreement between fits of eqs 18 to the data accessible by NR and SANS (Table 3). We thus can evaluate A and B as a function of the copolymer composition x, as shown by the solid lines in Figure 6 for a = 0.64 nm and a = 0.84 nm.

Taking into account the uncertainty in the mean segment length a, the fit functions of parts A and B of Figure 6 according to eq 18 are given for a = 0.64 nm by eq 19a and for a = 0.84 nm by eq 19b:

$$A(x) = (0.106 \pm 0.004) + (0.05 \pm 0.02)x - (0.19 \pm 0.02)x^2$$
$$B(x) = -(57.3 \pm 2.2) + (6.5 \pm 8.5)x + (68.8 \pm 8.3)x^2 \quad (19a)$$

$$A(x) = (0.105 \pm 0.005) + (0.09 \pm 0.02)x - (0.26 \pm 0.02)x^2$$
$$B(x) = -(56.7 \pm 1.7) - (13.0 \pm 6.7)x + (99.9 \pm 6.5)x^2 \quad (19b)$$

The agreement of the parabolic behaviour for A and B in theory and experiment justifies an analysis of the different χ-parameters involved in eq 15. They are listed in Table 4.

For the case of infinite degree of polymerization the spinodal is defined by $\chi(x,T) = 0$. The spinodal temperature T_s is then accessible from eq 17:

$$T_S = -B(x)/A(x) \quad (20)$$

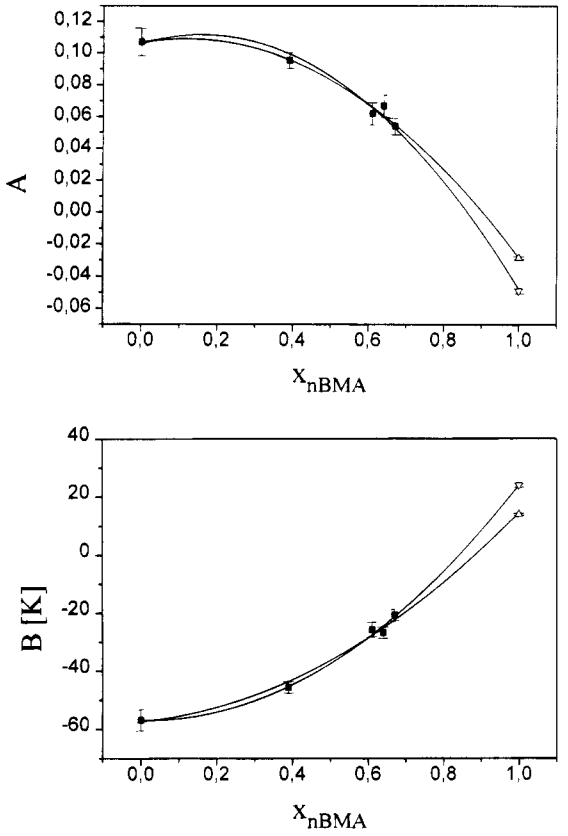

Figure 6. A and B (Table 3) as functions of copolymer composition. The solid lines correspond to parabolic fits based on eq 18 (NR data: a = 0.64 nm (△), a = 0.84 nm (▽); SANS data (■)). For details see text.

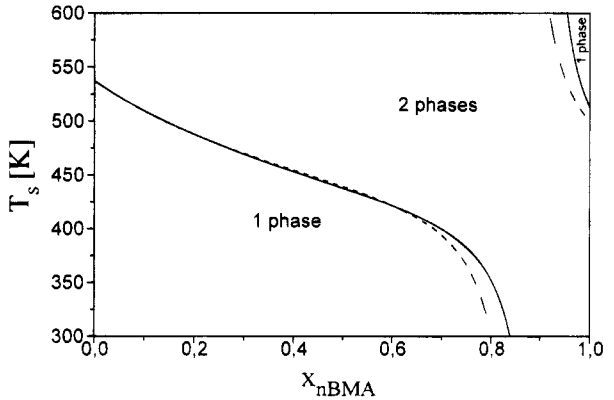

Figure 7. Spinodal temperature of PS(D)/P(CHA_{1-x}-*stat*-$nBMA_x$) as a function of the fraction x of nBMA in the copolymer calculated for the case of infinite degree of polymerization using eqs 19 and 20 (a = 0.64 nm (solid lines) and a = 0.84 nm (segmented lines)).

Table 4. Interaction Parameters for the Different Monomer Interactions According to Equation 15 (Calculated from Equation 19)

	a = 0.64 nm		a = 0.84 nm	
	A	B (K)	A	B (K)
χ_{S-nBMA}	−0.035	18.0	−0.060	30.1
χ_{S-CHA}	0.106	−57.3	0.105	−56.7
$\chi_{CHA-nBMA}$	−0.193	68.8	−0.258	99.9

Using eqs 19 and 20, one can calculate the phase diagram for the symmetric blend (Figure 7).

It is interesting to note that this analysis predicts a stronger incompatibility for blends where the copolymer contains 10−20% of CHA, as compared to blends of PS(D) and pure PnBMA. This is caused by the $\Delta\chi$ effect as expressed in eq 15. One can see from Table 4 that the χ-parameter for PnBMA and PCHA decreases with increasing temperature, which means that enthalpic interactions between the different segments become more favorable with increasing temperature. So, blends of PnBMA and PCHA should show an UCST behavior. The UCST behavior can be further understood, if the van der Waals volumes of both ester side groups are compared with each other. They deviate by about less than 20% from each other.[33] This leads to an UCST behavior of such a system, with the entropy being the driving force of miscibility as has been described in a more general way before.[4,34] We also predict a one-phase region at high temperatures (UCST) for a blend of PS and PnBMA of infinite molecular weight. It has been recently confirmed that UCST behavior is present for low molecular weight blends of those materials,[32] thus confirming this prediction.

Conclusions

By a combination of SANS and NR experiments from blends of PS(D) and P(CHA_{1-x}-*stat*-$nBMA_x$) the thermodynamics of mixing is investigated. By a variation of the copolymer composition the miscibility is largely changed. SANS experiments allow the determination of the Flory−Huggins−Staverman χ-parameter of blends in the one-phase region, while a measurement of the interface width in incompatible polymer blends by NR can be used to obtain a temperature-dependent χ-parameter also in the two-phase region. Both techniques together thus can cover the whole composition and miscibility range. χ turns out to be a linear function of $1/T$ in the accessible temperature range. From the copolymer composition dependence of χ, the individual interaction parameters between the different monomers of the copolymer and styrene as well as the intrinsic interaction parameter between the different comonomers are obtained and a prediction of the phase diagram becomes possible. As a result the transition from a LCST behaviour with a miscible regime at low temperatures and a two-phase regime at high temperatures to an UCST behavior is predicted, when the nBMA content is increased. Thermodynamics of this blend system is thus quite comprehensively understood within a mean-field approach. However, the determination of the χ-parameter from neutron reflectivity measurements needs the knowledge of the mean segment length of the system, which contains a rather large uncertainty in this case. Similarly other contributions to the interface width, e.g., from capillary waves and conformational effects, are not well understood and are neglected in present theories. But despite these problems the drawn picture of the phase behavior of this blend system should represent a reasonable approximation. While the temperature and copolymer composition dependence of χ can be phenomenologically described, a detailed molecular understanding of the segmental interaction is, of course, still missing. The measurement of monomer interaction parameters of different systems will help for that purpose.

The systematic study of a blend system with "adjustable" segmental interaction via statistical copolymerization of compatible and incompatible monomer components thus provides further insight into the problem of polymer miscibility. The combination of SANS and NR for those blends yields additional and new information in particular also for the two-phase region.

Acknowledgment. The authors thank Th. Wagner (Max-Planck-Institut für Polymerforschung) for the synthesis of deuterated polystyrene, V. Bartels (Max-Planck-Institut für Polymerforschung), and Dr. K. Mortensen (Risø, Denmark) for their assistance during the SANS measurements and B. Derichs (Max-Planck-Institut für Polymerforschung) for her assistance during the NR measurements. Neutron reflectivity experiments were performed within a collaboration agreement between GKSS and Max-Planck-Institut für Polymerforschung. Financial supports by Bundesministerium für Wirtschaft (AiF Grant No. 7695), by Bundesministerium für Forschung und Technologie (Grant NO. FI3MPG), and the European Community Large Installation Programme are gratefully acknowledged. V.A. also gratefully acknowledges a fellowship from the European Community Human Capital and Mobility Programme (No. ERBCHBICT930368).

References and Notes

(1) Olabisi, O.; Robeson, L. M.; Shaw, M. T. *Polymer-Polymer Miscibility*; Academic Press: New York, 1979.
(2) Utracki, L. A. *Polymer Alloys and Blends*; Hanser Publishers: München, Germany, 1989.
(3) MacKnight, W. J.; Kang, H. S.; Karasz, F. E.; Koningsveld, R. Thermodynamic Stability of Copolymer Blends. In *Integration of Fundamental Polymer Science and Technology*; Kleintjens, L. A., Lemstra, P. J., Eds.; Elsevier: London, 1989; Vol. 3.
(4) Siol, W. *Makromol. Chem., Macromol. Symp.* **1991**, *44*, 47.
(5) ten Brinke, G.; Karasz, F. E.; MacKnight, W. J. *Macromolecules* **1983**, *16*, 1827.
(6) Beaucage, G.; Stein, R. S.; Koningsveld, R. *Macromolecules* **1993**, *26*, 1603.
(7) Beaucage, G.; Stein, R. S. *Macromolecules* **1993**, *26*, 1609.
(8) Kressler, J.; Kammer, H. W.; Schmidt-Naake, G.; Herzog, K. *Polymer* **1988**, *29*, 686.
(9) Nishimoto, M.; Keskkula, H.; Paul, D. R. *Polymer* **1989**, *30*, 1279.
(10) Zeman, L.; Patterson, D. *Macromolecules* **1972**, *5*, 513.
(11) Stamm, M. *Adv. Polym. Sci.* **1992**, *100*, 357.
(12) Stamm, M. Reflection of Neutrons for the Investigation of Polymer Interdiffusion at Interfaces. In *Physics of Polymer Surfaces and Interfaces*; Sanchez, I. C., Ed.; Butterworths–Heinemann: Boston, 1992; p 163.
(13) Russell, T. P. *Mater. Sci. Rep.* **1990**, *5*, 171.
(14) Kunz, K.; Stamm, M. *Makromol. Chem., Macromol. Symp.* **1994**, *78*, 105.
(15) Sauer, B. B.; Walsh, D. J. *Macromolecules* **1991**, *24*, 5948.
(16) Fernandez, M. L.; Higgins, J. S.; Penfold, J.; Ward, R. C.; Shackleton, C.; Walsh, P. J. *Polymer* **1988**, *29*, 1923.
(17) Guckenbiehl, B.; Stamm, M.; Springer, T. *Physica B* **1994**, *198*, 127.
(18) *Polymer Handbook*, 3rd ed.; Brandrup, J., Immergut, E. H., Eds.; John Wiley & Sons: New York, 1989.
(19) Binder, K. *J. Chem. Phys.* **1983**, *79*, 6387.
(20) Anastasiadis, S. H.; Gancarz, I.; Koberstein, J. T. *Macromolecules* **1988**, *21*, 2980.
(21) Flory, J. P. *J. Chem. Phys.* **1941**, *9*, 660; **1942**, *10*, 51; **1944**, *12*, 425.
(22) Staverman, A. J. *Recl. Trav. Chim. Pays-Bas* **1941**, *60*, 640.
(23) Huggins, M. L. *J. Chem. Phys.* **1941**, *9*, 440.
(24) Koningsveld, R.; Šolc, K. *Collect. Czech. Chem. Commun.* **1993**, *58*, 2305.
(25) Lekner, J. *Theory of Reflection*; Martinus Nijhoff Publishers: Amsterdam, The Netherlands, 1987.
(26) Stamm, M.; Schubert, D. W. *Annu. Rev. Mater. Sci.*, to be published.
(27) Binder, K.; Frisch, H. *Macromolecules* **1984**, *17*, 2928.
(28) Stamm, M.; Hüttenbach, S.; Reiter, G.; Springer, T. *Europhys. Lett.* **1991**, *14*, 451.
(29) Helfand, E.; Sapse, A. M. *J. Chem. Phys.* **1975**, *62*, 1327.
(30) Kirste, R. G. *Makromol. Chem.* **1967**, *101*, 91.
(31) Ballard, D. G. H.; Wignall, G. D.; Schelten, J. *Eur. Polym. J.* **1973**, *9*, 965.
(32) Hammouda, B.; Bauer, B. J.; Russell, T. P. *Macromolecules* **1994**, *27*, 2357.
(33) Bondi, A. *J. Phys. Chem.* **1964**, *68*, 441.
(34) Siol, W.; Terbrack, U. U.S. Patent 4900791, 1990.

MA945046P